ISSN 2176-5480

22nd International Congress of Mechanical Engineering (COBEM 2013)
November 3-7, 2013, Ribeirão Preto, SP, Brazil

DYNAMIC AND CONTROL OF A ROTOR SYSTEM BASED ON PASSAGE THROUGH CRITICAL SPEEDS WITH INCORPORATION OF SMART ACTUATORS IN FLEXIBLE BEARING DEVICE

Richard Senko
Federal University of Campina Grande, Rua Aprígio Veloso, Campina Grande-PB, Brazil
senko.richard@gmail.com
Antonio Almeida Silva
Federal University of Campina Grande, Rua Aprígio Veloso, Campina Grande-PB, Brazil
almeida@dem.ufcg.edu.br
Jader Morais Borges
Federal University of Campina Grande, Rua Aprígio Veloso, Campina Grande-PB, Brazil
jader@dem.ufcg.edu.br

Abstract. *Rotor machines are rather simply, thus obtains a wide application in several industrial areas. Researches about rotors seek to avoid the vibrations that occur when it is in critical operation conditions, which can damage other devices that are connected. The objective of this paper is realize rotor dynamics comportment analysis using simulations, working with finite elements, achieving curves and comparing with experimental setup, where it can have two types of setups, with two rigid bearings and another with one rigid and other flexible bearing using springs with shape memory alloy. The simulations were derived via computer programs such as Matlab platform, which was obtained by finite element analyzes and curves in time and frequency, and ANSYS, where can obtain the deformation the material may suffer during test conditions. The experimental data were achieved through equipments of dynamic analysis and computers connected by sensors in experimental bench. We can conclude that analysis of that system can be appropriate to control, prevention and maintenance of this rotating devices, so as to achieve a decrease of costs to industry.*

Keywords: *Vibration control, Rotor machines, Dynamics analysis, Finite elements, Shape memory alloy.*

1. INTRODUCTION

Rotating machines are used in many applications, having the rotor is the simplest. Following the ISO definition, rotor is a body suspended by a set of roller bearings, that allows it to rotate freely about a fixed axis in space. According to Pereira (2003), the capacity to transmit high energies being a small equipment is of great interest, where this energy comes from the high speed at which the rotor bearing system may be subjected. The rotor bearing system is usually constituted basically of the following elements: shaft, bearing and disc. The disc can be assumed as a rigid element, which is characterized only by kinetic energy. The disc is located where the rotor undergoes the highest amplitudes during rotation of the system. In some instances the rotor may have more than one disc. The shaft is usually circular and symmetrical, and is mounted with the disc, supported on bearings. It is characterized by kinetic and potential energy, getting the parameters of stiffness, mass and damping. The bearings represent the points where the shaft will be supported, and it can be divided by balls, rollers, hydrodynamic or aerostatic bearings. The bearings are characterized by the virtual work of the forces acting on the shaft, which due to contact both generate forces of restitution in the bearing. The unbalanced mass, is characterized by kinetic energy, it is usually related to the disc itself. By more than unbalanced mass is not an element of the rotor, but it can be used to correct unbalances, thereby reducing the vibration system.

A representation of this assembly contains the shaft, disc and bearings (rigid and flexible) is illustrated in Fig. 1. Also is considered some residual unbalance in the system.

ISSN 2176-5480

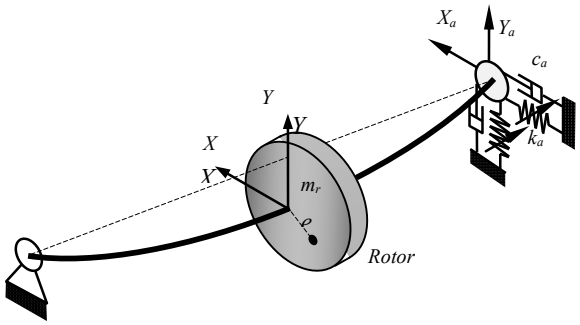

Figure 1. System axis-rotor-bearing (adapted by He *et al*., 2007)

The unbalance is the greatest cause of vibrations in rotating machines and this phenomenon is characterized by the existence of unbalanced mass in relation to the axis of rotation (Lamin Brito, *et al*., 2006). Such unbalances are caused by inevitable asymmetries, tolerances and deviations in shape, in addition to the imperfections of the raw material and assembly.

When the system is unbalanced can generate undesirable behaviors, which can cause extensive damage to other equipments that are interconnected.

Thus arises the need to study the dynamics of rotors for a better understanding of vibration signals and achieve improved models for the system. Therefore the method of finite element is quite attractive due to close approximation of reality models. The utilization of smart materials for rotor systems is of particular interest since they can provide better performance while avoiding many undesirable behaviors. Silva *et al*. (2012), show that shape memory alloys (SMAs) represent an interesting alternative where adaptive characteristics and high dissipation capacity are required.

Borges *et al* (2012) currently has studied the application of new materials made from special alloys, such as actuators for dynamic systems in order to reduce the vibrations in a frequency range due to the resonance region. In this regard, the use of components of active materials such as Smart Memory alloys (SMA) which are "smart", capable of regaining its original shape when the temperature change and/or mechanical stress and, the main characteristic, a high capacity variation of the stiffness and damping can be incorporated to attenuate the vibration.

Therefore this paper aims to analyze the rotor dynamics simulations using a dedicated system, obtaining the curves of frequency response and corresponding amplitudes. The main motivation is to explore the methods implemented in computer simulations, in order to compare the data obtained in the experimental setup, where it can have two sets of bearings, rigid bearing and another with a flexible bearing using SMA springs.

2. MATHEMATICAL MODELING

To perform the simulations is necessary to obtain the mathematical model of the rotor-bearing system, where was used Finite Element Method. Initially it was found the kinetic energy, potential and forces that were applied to the elements of the system, as described by Lalanne (1990).

2.1 Finite Elements Method

According to Rao (2011), this methods allow more accurate predictions, reducing the cost of experiments and simulation, thus achieving cheaper and more accurate designs before testing prototypes. Through this method can be found matrices of mass, stiffness, damping, the gyroscopic effect mass and unbalanced. In this method is used the energy equations for each element, and without the generalized coordinates, but with the degrees of freedom available in the element. For the derivation of the equations of motion of the rotor, just apply the Lagrange equation in the kinetic energy, potential and forces the system. The general equation is given as:

$$\frac{d}{dt}\left(\frac{\partial T}{\partial \dot{\delta}}\right) - \frac{\partial T}{\partial \delta} + \frac{\partial U}{\partial \delta} = F\delta \tag{1}$$

Where ($1 \leq i \leq N$) is the numbers of degree of freedom, δ is the displacement vector and º indicates differentiation in relation to time. These equation follows a procedure used by Santiago (2003). In the case of the disc element, as it has four degrees of freedom, *u, w, θ*, and *ψ*, Fig. 2:

ISSN 2176-5480

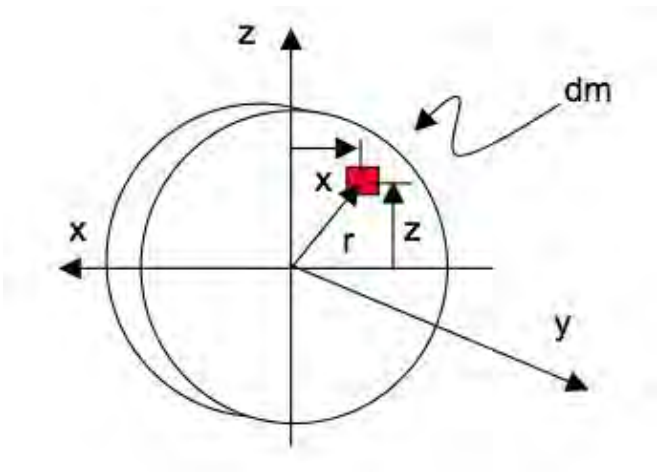

Figure 2. Representation of disk (Pereira 2003)

Assuming that the kinetic energy of the disc is obtained using Lagrange has to the following equation:

$$\frac{d}{dt}\left(\frac{\partial T_D}{\partial \delta'}\right) - \frac{\partial T_D}{\partial \delta} = [M_D]\{\delta''\} + \Omega[C_D]\{\delta'\} \tag{2}$$

where $[M_D]$ is the classical mass matrix and $[C_D]$ is the gyroscopic matrix.
To shaft matrices, first is shown that this have to be divided through nodes, as shown in Fig. 3:

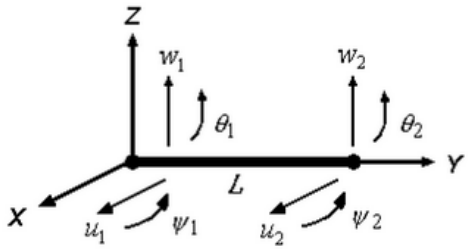

Figure 3. Representation of shaft. (Lalanne, 1990)

Through Fig. 3, it can be noted that each node has four degrees of freedom thus forming the nodal displacement vector. Knowing that the displacements ψ and θ are derivations of u and w, with this information, and according to Fish and Belytschko (2007), is obtained the shape functions of the element shaft. The equation for kinetic energy of the shaft is given by:

$$T_S = \frac{\rho S}{2}\int_0^L \left[\delta\dot{u}^T N_1^T N_1 \delta\dot{u} + \delta\dot{w}^T N_2^T N_2 \delta\dot{w}\right]dy + \frac{\rho I}{2}\int_0^L \left[\delta\dot{u}^T \frac{dN_1^T}{dy}\frac{dN_1}{dy}\delta\dot{u} + \delta\dot{w}^T \frac{dN_2^T}{dy}\frac{dN_2}{dy}\delta\dot{w}\right]dy$$
$$-2\rho I\Omega \int_0^L \delta\dot{u}^T \frac{dN_1^T}{dy}\frac{dN_2}{dy}\delta w dy + \rho IL\Omega^2 \tag{3}$$

where ρ is the density, S transversal area, N_1 and N_2 shape functions, I inertia moment, Ω angular velocity and L length. Making the necessary integrations and applying Lagrange, is obtained:

$$\frac{d}{dt}\left(\frac{\partial T_S}{\partial \delta'}\right) - \frac{\partial T_S}{\partial \delta} = [M + M_S]\{\delta''\} + \Omega[C_S]\{\delta'\} \tag{4}$$

where $[M]$ is the classical mass matrix, $[M_S]$ effect of inertia matrix and $[C_S]$ gyroscopic matrix.
To potential energy, have to make the same procedure:

ISSN 2176-5480

$$U = \frac{EI}{2}\int_0^L \left[\delta u^T \frac{d^2N_1^T}{dy^2}\frac{d^2N_1}{dy^2}\delta u + \delta w^T \frac{d^2N_2^T}{dy^2}\frac{d^2N_2}{dy^2}\delta w\right] dy + \frac{F_0}{2}\int_0^L \left[\delta u^T \frac{dN_1^T}{dy}\frac{dN_1}{dy}\delta u + \delta w^T \frac{dN_2^T}{dy}\frac{dN_2}{dy}\delta w\right] dy \quad (5)$$

where E is the elasticity modulus and F_0 external force.
Making the necessary integrations and applying Lagrange, is obtained:

$$\frac{\partial U}{\partial \delta} = [K_c + K_F]\delta \quad (6)$$

where $[K_C]$ is the classical stiffness matrix and $[K_F]$ axial force matrix.

As for bearing is simpler to find the matrix, because having the force equation, the matrix is obtained directly:

$$\begin{bmatrix} F_u \\ F_\theta \\ F_\omega \\ F_\psi \end{bmatrix} = -\begin{bmatrix} k_{xx} & 0 & k_{xz} & 0 \\ 0 & 0 & 0 & 0 \\ k_{zx} & 0 & k_{zz} & 0 \\ 0 & 0 & 0 & 0 \end{bmatrix}\begin{bmatrix} u \\ \theta \\ \omega \\ \psi \end{bmatrix} - \begin{bmatrix} c_{xx} & 0 & c_{xz} & 0 \\ 0 & 0 & 0 & 0 \\ c_{zx} & 0 & c_{zz} & 0 \\ 0 & 0 & 0 & 0 \end{bmatrix}\begin{bmatrix} u' \\ \theta' \\ \omega' \\ \psi' \end{bmatrix} \quad (7)$$

Considering the first the matrix of stiffness and the second matrix of damping, where they can be symmetric, when $k_{xx} = k_{zz}$ e $c_{xx} = c_{zz}$, or asymmetric when $k_{xx} \neq k_{zz}$ e $c_{xx} \neq c_{zz}$.
In the case of unbalanced mass matrix is also obtained directly, applying the Lagrange in the equation kinetic energy of the unbalanced mass, we obtain the following matrix.

$$\begin{bmatrix} F_u \\ F_\omega \end{bmatrix} = m_u d\Omega^2 \begin{bmatrix} \cos(\Omega t + \alpha) \\ \sin(\Omega t + \alpha) \end{bmatrix} \quad (8)$$

where Ω is the angular velocity and α is the angular position with respect z axis.

3. MATERIALS AND METHODOLOGY

3.1 Materials

Was used data and geometric parameters of the experimental setup existent in LVI (Laboratory of Vibration and Instrumentation - UAEM / UFCG), Fig. 4, which is composed of a system rotor shaft bearing, which is assumed initially that bearings are rigid. The system also features a frequency inverter, *Mline WEG*, and motor, *WEG W22 plus*, it has the maximum speed of 3330 rpm. Data for experimental setup are shown in Tab.1 and Tab. 2.

Figure 4. Experimental setup (LVI-UAEM-UFCG)

ISSN 2176-5480

Table 1. Disk and shaft data.

	Disk	Shaft
Mass	2.107 kg	0.30 kg
Position	0.21 m	-
D_{in}	0.0126 m	0
D_{out}	0.15 m	0.0126 m
Length	-	0.42 m
Thickness	0.0171 m	-
Stiffness	-	1.6527 E5 N/m
Damping	-	2.3 E-4 N s/m

Table 2. Bearings and unbalanced mass data.

	Bearing	Unbalanced Mass
Mass	-	0.001 kg
Position	l_2=0 ; l_3=0.42 m	0.21 m
Stiffness	k_{xx}=k_{zz}=2.22 E6 N/m	-
Damping	c_{xx}=c_{zz}=2.84 N s/m	-
Stiffness (Martensite)	k_{xx}=k_{zz}=11049 N/m	-
Damping (Martensite)	c_{xx}=c_{zz}=10 N s/m	-
Stiffness (Austenite)	k_{xx}=k_{zz}=16976 N/m	-
Damping (Austenite)	c_{xx}=c_{zz}=5 N s/m	-

3.2 Methodology

For simulations were used as computational software *Ansys* and *Matlab* where the methods and data presented experimental setup use three different bearings configurations:

- Bearings Rigid-Rigid
- Bearings Rigid-SMA Martensite
- Bearings Rigid-SMA Austenite.

To apply in the *Matlab* the finite element method, was implemented subroutines of the program and the shaft was divided into 5 nodes and the placement of these nodes placed symmetrically. The program also requires the placement of the disc and bearings, which was thus obtained a close approximation of the actual model.

For software *ANSYS*, it was necessary to use the modulus of elasticity, Poisson's ratio and density of the shaft. For the disc is inserted the mass, inertia polar and diametrical. In case the bearing was only necessary damping and stiffness data. Thus the system was divided into 10 elements, where the shaft is partitioned into 11 nodes symmetrically, and 8 more were included the springs bearing, following the model used by Lalanne (1990).

At this software was performed modal analysis and harmonic excitation, where in the latter was included a mass unbalanced on disc, at a distance equal to the radius of the disc relative to the center, and simulating the system with a rotation speed of 50Hz because this rotation it passes through the first natural frequency.

The modal analysis experiments were made using impact tests with instrumented hammer and the dynamic signal analyzer *35679A Agilent* , Fig. 5, consisting of:

- Accelerometer (PCB 3528B10 SN 34589);
- Impact hammer (PCB 086C03); Maximum voltage 20-30 VDC, maximum strength 2224 N (pk), sensitivity 2.25 mV/N, resonance frequency exceeding 22.5 kHz.

ISSN 2176-5480

Figure 5. Instrumentation of dynamic signal analysis.

For modal testing the system has been maintained static and to perform analyzes the accelerometer was placed in the left bearing in horizontal and vertical directions and the impact hammer was given on disc, because it is the center position of the rotor and the point which suffers the highest amplitudes. In this experiment were obtained response curves in the time and frequency. After all the data obtained through each method, was performed a comparison of results, to thereby, evaluate what criterion was the closest experimental tests for system validation. Fig. 6 illustrate a schematic representation of the procedure followed.

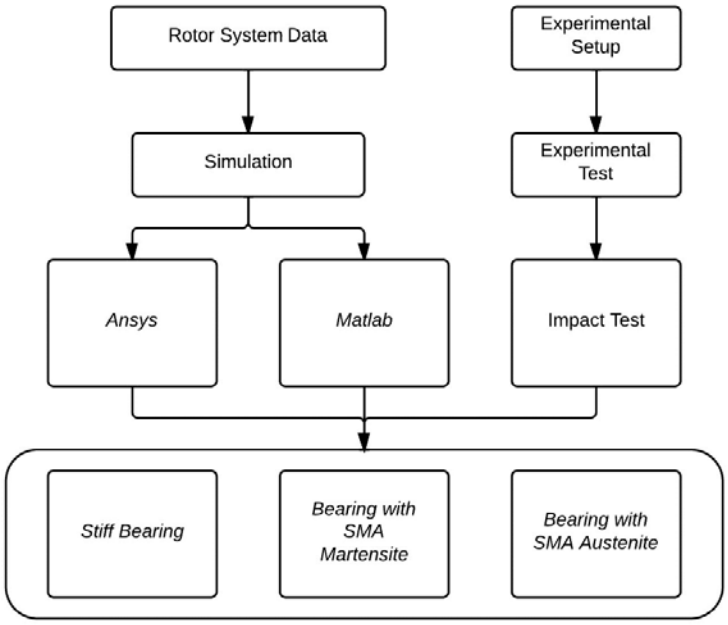

Figure 6. Schematic representation of the analysis.

4. RESULTS AND DISCUSSIONS

For simulations by finite element following programs were used, *Matlab* and *Ansys*. In the first program, all data, Tab. 1 and Tab. 2, from the experimental setup, Fig. 4, were inserted. Thus was possible to obtain the following curves (Fig 7, 8 and 9), is possible to note the differences in stiffness for the three cases, just analyzing the amplitudes on the bearings in all figures of vibrations modes:

ISSN 2176-5480

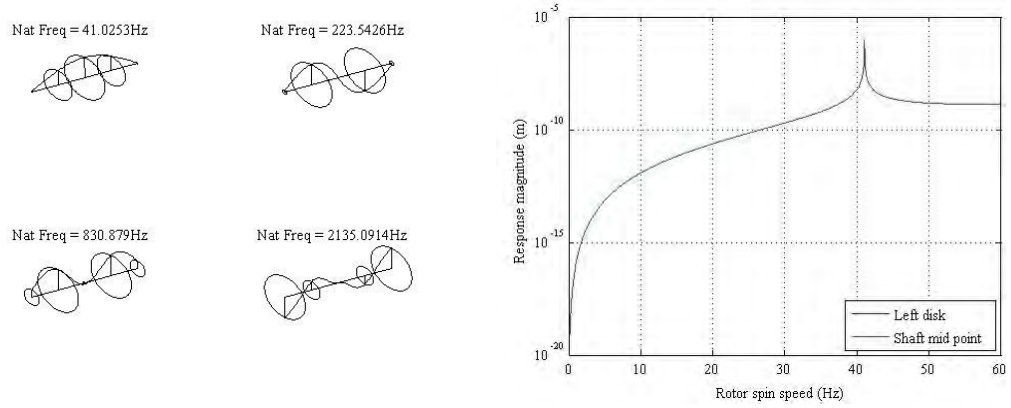

Figure 7. (a) Vibrations modes; (b) response curve with unbalanced mass, *Matlab*.

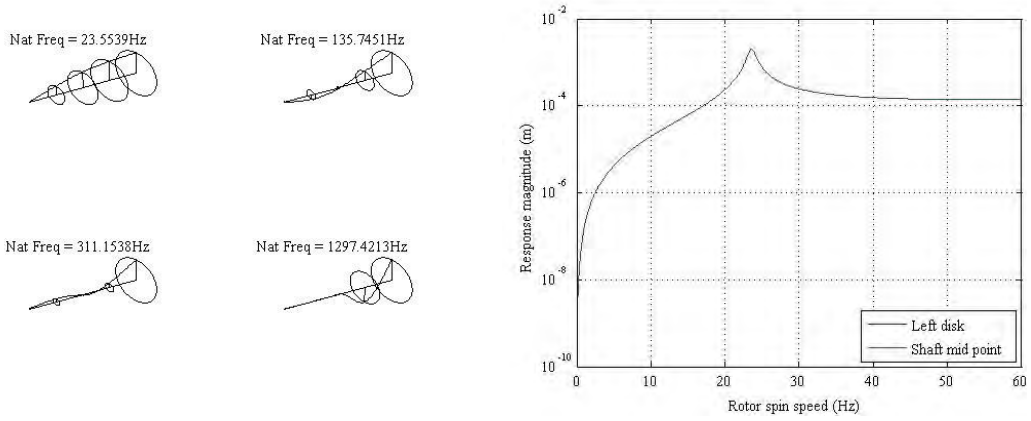

Figure 8. Bearing with SMA martensite (a) Vibrations modes; (b) response curve with unbalanced mass, *Matlab*.

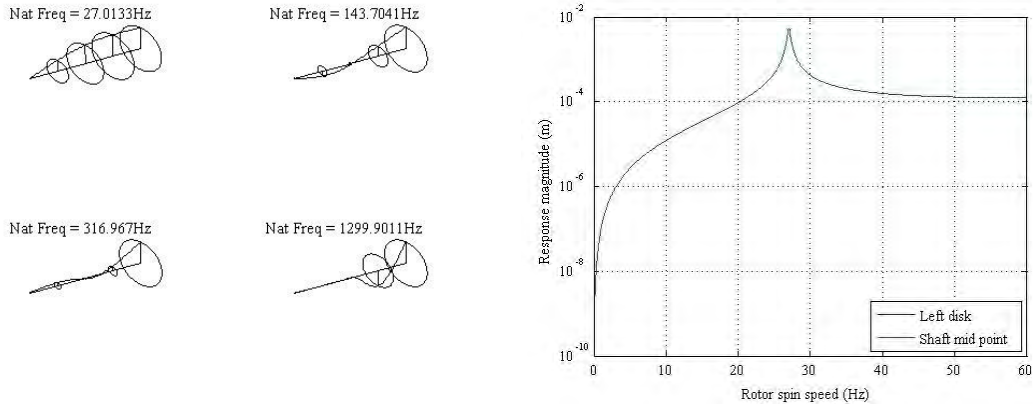

Figure 9. Bearing with SMA austenite (a) Vibrations modes; (b) response curve with unbalanced mass, *Matlab*.

For *Ansys*, after entering all necessary data previously described, we performed a modal analysis thus obtaining the first three vibration modes of the system, as shown in Tab 3, 4 and 5.

After the modal analysis was performed harmonic analysis and thus obtained the frequency response curve, as shown in Fig. 10.

ISSN 2176-5480

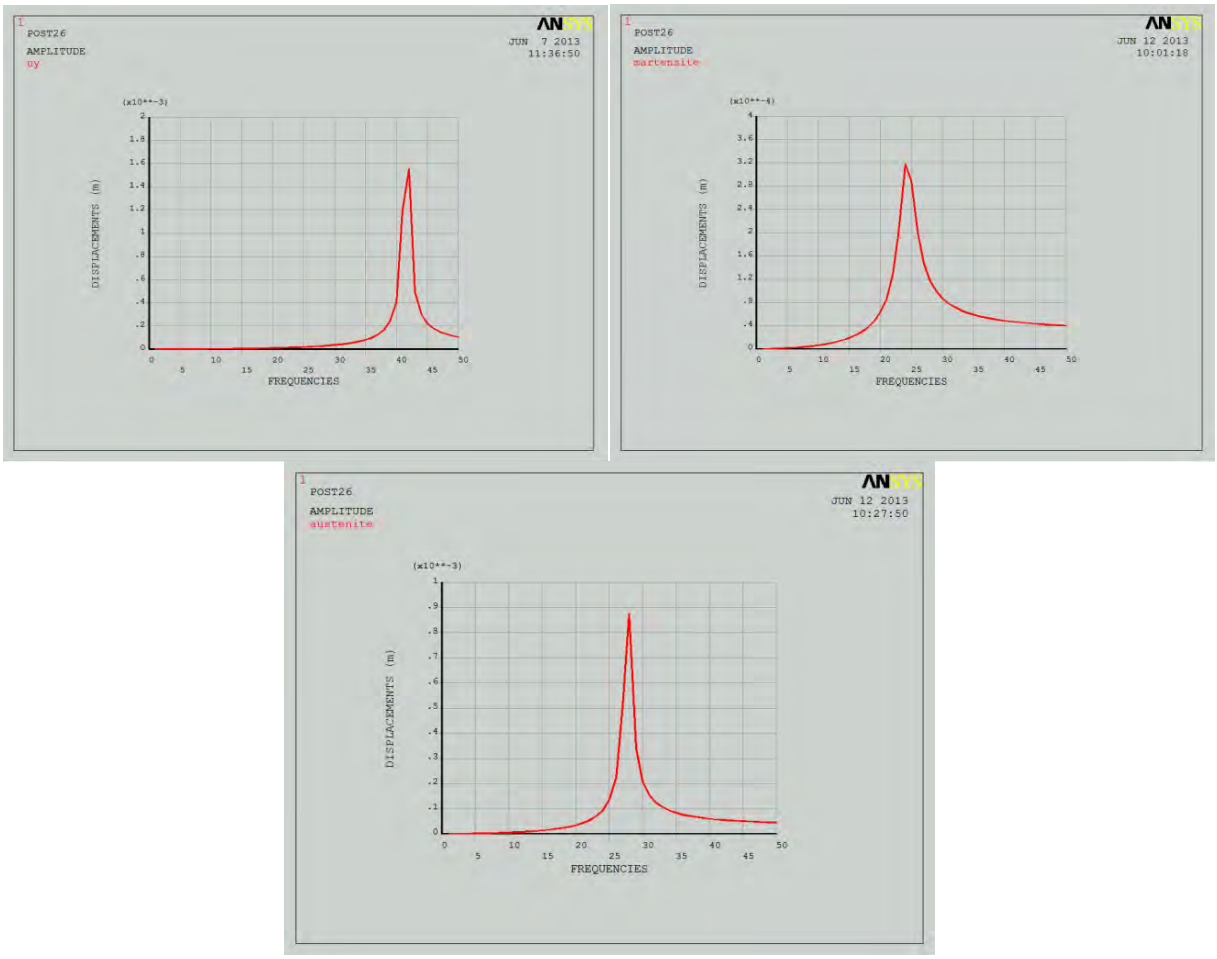

Figure 10. Response curve with unbalanced mass applied; (a) Rigid bearing; (b) Bearing with SMA martensite phase; (c) Bearing with SMA austenite phase, *Ansys*.

Having the simulation results began experimental tests to compare the results. After performing the test, the data were placed in *Matlab* in order to obtain a better view. Was obtained a curve of the free vibration response time and the respective frequency response.

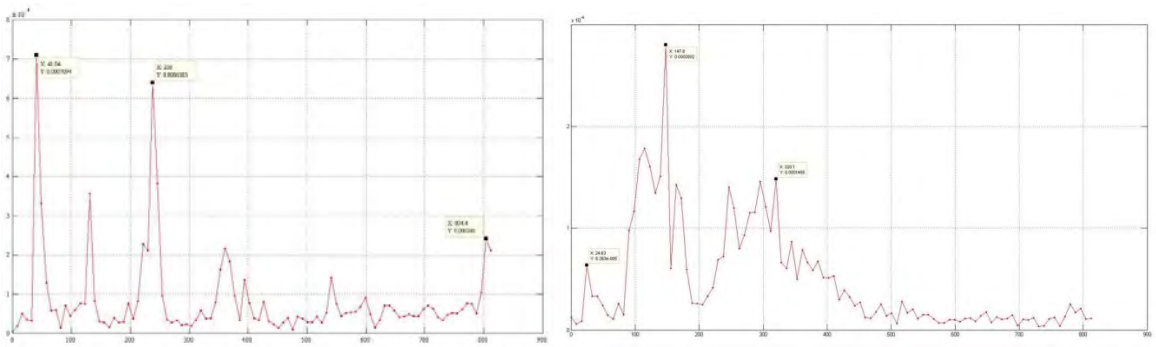

ISSN 2176-5480

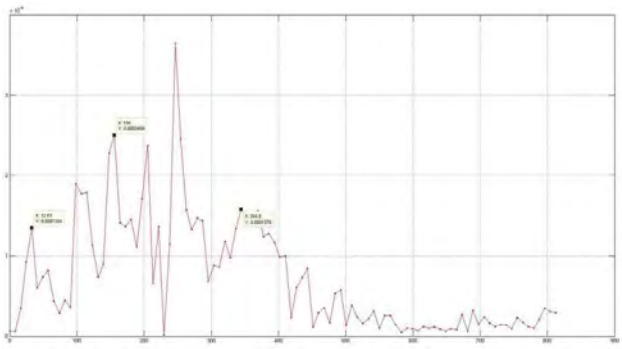

Figure 11. Experimental response with dynamic signal analyzer response in frequency (a) Rigid bearing; (b) Bearing with SMA martensite phase; (c) Bearing with SMA austenite phase.

The difference between the natural frequencies shown in curves is due the bearings, because was tested three cases, with rigid bearing, Figs. 7, 10(a) and 11(a), and two flexible bearings, one using a SMA in martensite phase, Figs. 8, 10(b) and 11(b), and another one using SMA in austenite phase, Fig. 9, 10(c) and 11(c). In this case the stiffness of each one is different, being the rigid bearing stiffer than others. Therefore the natural frequency is highest. The bearing with SMA in martensite phase is the more flexible, because it has the lowest stiffness and natural frequency.

Obtained all results, simulated and experimental, a comparison was made between the natural frequencies and the corresponding vibration modes between different methods adopted, as Tabs. 3, 4 and 5.

Table 3. Natural frequencies with bearing.

	Ansys Hz	Matlab (FEM) Hz	Experimental Hz	Error (%)	
				Ansys x Matlab	Ansys x Experimental
Wn (1ª mode) Hz	41.56	41.02	41.04	1.29	1.24
Wn (2º mode) Hz	237.76	223.54	238.00	5.98	0.10
Wn (3º mode) Hz	821.51	830.87	804.40	1.14	2.08

Table 4. Natural frequencies with bearing SMA martensite phase.

	Ansys Hz	Matlab (FEM) Hz	Experimental Hz	Error (%)	
				Ansys x Matlab	Ansys x Experimental
Wn (1ª mode) Hz	23.98	23.55	24.63	1.79	2.71
Wn (2º mode) Hz	139.43	135.75	147.80	2.64	6.00
Wn (3º mode) Hz	322.50	311.15	320.10	3.52	0.74

Table 5. Natural frequencies with bearing SMA austenite phase.

	Ansys Hz	Matlab (FEM) Hz	Experimental Hz	Error (%)	
				Ansys x Matlab	Ansys x Experimental
Wn (1ª mode) Hz	27.50	27.01	27.09	1.78	1.47
Wn (2º mode) Hz	148.15	143.70	156.00	3.00	5.30
Wn (3º mode) Hz	327.50	316.97	344.80	3.22	5.28

Thus it can be seen positive results, obtaining small errors on the order of up to 2% compared to the first natural frequency obtained by the methods used. Thus it can be noticed that the methods used and the simulations are consistent with the physical model. The differences between simulations and experimental in flexible bearing cases, can be because of the bearing stiffness, due to difficulty to use the number of turns compatible with the stiffness calculated.

5. CONCLUSIONS

This paper presented a dynamic study of a rotor-bearing system dedicated, using data from an experimental setup that is available in the LVI-UAEM-UFCG, aiming to obtain important parameters such as natural frequencies and mode shapes when subjected to three different configurations. At a later stage aims to implement a system of vibration control

ISSN 2176-5480

while passing by one of these critical frequencies. Analyzing and comparing the simulated results obtained with the experimental analysis, we obtained quite satisfactory results with small margin of error, especially for the first mode. The largest margin of error for the other two modes can be justified because the conditions applied in the simulation, which was treated both bearings identical, with equal stiffness in the directions x and z. In the experimental setup bearings contains greater stiffness in the vertical direction than in the horizontal, and are different due to their geometry.

6. ACKNOWLEDGEMENTS

The authors would like to thank the Academic Unit of Mechanical Engineering from Federal University of Campina Grande for the opportunity to using the Dynamic and Vibration Laboratory (LVI) and Multidisciplinary Laboratory of Active Materials and Structures (LaMMEA), and CNPQ.

7. REFERENCES

Borges, J. M., Silva, A. A., Araújo, C. J., Fernandes, E. M., Pimentel, R. L. and Santiago, A. A., 2013. “A Rotor-bearing vibration control system based on fuzzy controller and smart actuators”. *The International Journal of Multiphysics*. Vol. 7, N. 3, p. 197-205.

Fish, J., Belytschko, T., 2007. *A First Course in Finite Elements*, John Wiley and Sons, 319p.

He. Y., Satoko, O., Chu, F. L. and Li, H. X., 2007. Vibration control of a rotor-bearing system using shape memory alloy: I – Theory, *Smart Materials and Structures*, Vol. 16, pp. 114-121.

Lalanne, M., Ferraris, G., 1990. *Rotordynamics prediction in engineering*, John Wiley and Sons, 198p.

Lamim Filho, P. C. M., Pederiva, R., Brito, J. N., 2006. "Detecção de Desbalanceamento em máquinas rotativas através da lógica fuzzy". In: *Anais do IV Congresso Nacional de Engenharia Mecânica - CONEM 2006*, Recife - PE.

Pereira, J. C., 2003. *Introdução à Dinâmica de Rotores***,** Florianópolis.

Rao, J. S., 2011. *History of Rotating Machinery Dynamics*, Springer, 380p.

Santiago, D. F. A., 2003. *Diagnostic of faults of rotating machinery using wavelet transform and artificial neural networks*. Phd Thesis, am inas acu ldade de ngen aria e c nica, Universidade Estadual de Campinas, 117 p.

Silva, L. C., Savi, M. A., Paiva, A., 2013. "Nonlinear Dynamics of a Rotordynamic Nonsmooth Shape Memory Alloy System". *Journal of Sound and Vibration*, v. 332, p. 608-621.

8. RESPONSIBILITY NOTICE

The authors are the only responsible for the printed material included in this paper.